APPLICATIONS PAPER

Remote Sensing of Tamarisk Biomass, Insect Herbivory, and Defoliation: Novel Methods in the Grand Canyon Region, Arizona

Temuulen Ts. Sankey, Joel B. Sankey, Rene Horne, and Ashton Bedford

Abstract

Tamarisk is an invasive, riparian shrub species in the southwestern USA. The northern tamarisk beetle (Diorhabda carinulata) has been introduced to several states to control tamarisk. We classified tamarisk distribution in the Glen Canyon National Recreation Area, Arizona using 0.2 m resolution, airborne multispectral data and estimated tamarisk beetle effects (overall accuracy of 86 percent) leading to leaf defoliation in a 49,408 m^2 area. We also estimated individual tamarisk tree biomass and their uncertainties using airborne lidar data (100 points/m^2). On average, total aboveground tamarisk biomass was 8.68 kg/m2 (SD = 17.6). The tamarisk beetle defoliation resulted in a mean leaf biomass loss of 0.52 kg/m^2 and an equivalent of 25,692 kg across the entire study area. Our defoliated tamarisk map and biomass estimates can help inform restoration treatments to reduce tamarisk. Continued monitoring of tamarisk and tamarisk beetle effects are recommended to understand the currently-unknown eventual equilibrium between the two species and the cascading effects on ecosystem processes.

Introduction

Saltcedar (*Tamarix ramosissima*), also known as tamarisk, was originally introduced from Asia to the United States in the late 1800's as a decorative tree that provided shade and wind break, and to prevent soil erosion (Crins, 1989). Tamarisk eluded the controlled cultivation, and was initially found in riparian areas close to the cultivation site. By the beginning of the 20th century, tamarisk was found in almost all of the Southwestern riparian areas, where the native woody vegetation consisted of cottonwood (*Populus fremontii*), willows (*Salix spp.*), and the western honey mesquite (*Prosopis glandulosa*) (Infalt, 2005). It was recently estimated to be spreading along the arid and semi-arid river systems across the western United States at a rate of 25 km per year (Nagler *et al.*, 2011).

Tamarisk tree has many biological adaptations that enable its successful invasion in arid ecosystems: (a) it outcompetes the native flora for water resources using its large tap roots that reach deeper sources of water (Hart, 2009), (b) tamarisk has a high germination rate: its small seeds can germinate within 24 hours of dispersal under wet conditions (DiTomaso, 1998), and (c) it accumulates salt in its leaves, which the tamarisk drops annually to maintain salty soil unhospitable for many native species (Ladenburger *et al.*, 2006; Glenn *et al.*, 2012; Ohrtman *et al.*, 2012; Merritt and Shafroth, 2012). River management and water cycle alterations including dam construction, flow regulation, flow diversion, flood control, and infrastructure for crop irrigation (DiTomaso, 1998) have further enhanced the invasive advantages for tamarisk. Many local, state, and federal agencies have targeted a great deal of management effort on tamarisk control. Chemical, mechanical, and prescribed fire control methods have been costly with mixed results (Jorgensen, 1996; Hultine *et al.*, 2010). A biological control, known as the northern tamarisk beetle (*Diorhabda carinulata* Desbrochers), has been determined to be an effective control agent (DeLoach *et al.*, 2003; Snyder *et al.*, 2010).

Prior to its introduction, the beetle was carefully considered for many important parameters (Pattison *et al.*, 2011) to confirm that it has a narrow host range with impact on the target species only and is effective in desired climatic conditions (Dudley *et al.*, 2012). Following many experiments, the beetle was introduced in 2001 to Colorado, Utah, Wyoming, Nevada, California, and Texas. The beetle was then introduced to Moab, Utah in 2005, and was not expected to travel south past 38 degrees North latitude due to temperature limitations (DeLoach *et al.*, 2003) and a dormancy cycle, known as diapause, associated with day lengths (Bean *et al.*, 2007; Dudley, 2005). In 2009, however, tamarisk beetle was found further south than anticipated in the Colorado River ecosystem within the Glen Canyon National Recreation Area and Grand Canyon National Park. Since then, the tamarisk beetle has spread at a more rapid rate than expected (Nagler *et al.*, 2014) throughout many reaches of the Colorado River with visible signs of herbivory on the tamarisk trees.

The tamarisk beetle preys on tamarisk by defoliating the leaves during the growing season and multiple times per year (Paxton *et al.*, 2011; Snyder *et al.*, 2010). Each cycle progressively weakens the plant. After several growing seasons of the repeated cycle, the tree can eventually die due to carbohydrate reserve depletion. The defoliation can happen over a large land area as the beetle population grows and disperses across the tamarisk stands (Paxton *et al.*, 2011; Snyder *et al.*, 2010). The wide range makes ground monitoring of beetle impact difficult, and often not very accurate. Remote sensing techniques have, therefore, been used to monitor beetle impacts (Dennison *et al.*, 2009; Nagler *et al.*, 2012; Nagler *et al.*, 2014; Meng *et al.*, 2012). As tamarisk leaves are defoliated, the leaves turn a noticeable brown-orange color, which is detectable in the visible and the near infrared spectrum in remote sensing data (Dennison *et al.*, 2009; Fletcher, 2013; Meng and Dennison, 2015). Furthermore, the leaf defoliation and the eventual tree mortality result in substantial decrease in photosynthetic activity and biomass (Bateman *et al.*, 2015),

Temuulen Ts. Sankey, Rene Horne, and Ashton Bedford are with the Informatics and Computing Program, Northern Arizona University, 1298 S. Knoles Drive, Flagstaff, AZ 86011, (Temuulen.Sankey@nau.edu).

Joel B. Sankey is with the US Geological Survey, Grand Canyon Monitoring and Research Center, Southwest Biological Science Center, 2255 N. Gemini Drive, Flagstaff, AZ 86001.

Photogrammetric Engineering & Remote Sensing
Vol. 82, No. 8, August 2016, pp. 645–652.
0099-1112/16/645–652

doi: 10.14358/PERS.82.8.645

which can be detected in vegetation indices such as the Normalized Difference Vegetation Index (NDVI) (Bateman *et al.*, 2013; Bateman *et al.*, 2015; Dennison *et al.*, 2009).

Ground-based and remote sensing estimates of tamarisk and beetle effects on tamarisk along the Colorado River in Glen and Grand Canyons are particularly important given the significance of the National Park Service Units and the unique land management effects of the tamarisk within the canyons (Cross *et al.*, 2011). Tamarisk is found in much of the riparian habitat along the Colorado River in the Grand Canyon with substantial impacts on wildlife and ecosystem services (Dennison *et al.*, 2009). The expansion of tamarisk on the floodplain has negatively impacted recreational activities, in particular camping, fishing, and boating along river beaches and sandbars (Penny, 1991).

We present here a remote sensing approach to mapping and monitoring total aboveground tamarisk biomass at the individual tree level across a large spatial extent. We further demonstrate the approach in estimating only the green leaf biomass portions of the individual trees which can be affected by tamarisk beetle herbivory and defoliate. This approach can be similarly used to monitor biomass of other tree species that can be affected by phenological events such as green-up and leaf-out phases as well as annual leaf defoliation, and herbivory. Tamarisk biomass measurements are important for invasive species management because they are used in planning restoration treatment activities such as mechanical removal and prescribed fire, and in estimates of ecosystem productivity, leaf area, and nutrient cycling (Evangelista *et al.*, 2007; Hultine *et al.*, 2010a and 2010b). Estimating tree biomass is always a challenge in any environment, especially across large areas. Commonly used, ground-based methods include destructive sampling or complete harvesting and allometric models of tree structural characteristics (e.g., diameter, height, and canopy area). Our approach leverages the combination of airborne, high point-density lidar data and airborne, high spatial resolution multitemporal, multispectral imagery. The hypothesis of this study is that the unique combination of these data would provide accurate and efficient estimates of tamarisk biomass and tamarisk beetle effects. The objectives of this study are to:

1. Develop a remote sensing method to estimate total aboveground tamarisk biomass as well as leaf-only tamarisk biomass using lidar and existing allometric relationships,
2. Demonstrate how the fusion of lidar and multitemporal, multispectral imagery can be used to monitor the effects of green leaf biomass defoliation,
3. Quantify the uncertainties associated with the above estimates in a robust manner that accounts for each of the key sources of uncertainty in riparian biomass estimates.

Methods

Study Area

Our study area spans the Colorado River within the Glen Canyon National Recreation Area which is just upstream of Grand Canyon National Park, Arizona (Plate 1). This section of the Colorado River spans 24 km between the Glen Canyon

Plate 1. The study area and major landmarks within the Grand Canyon region, Arizona. The background image is a US Geological Survey digital elevation model (DEM), which illustrates the topographic variability. The canyon and the Colorado River are shown in the multispectral data used in this study. The additional insets are examples of the airborne lidar data (A and B), healthy green tamarisk (C), and defoliated tamarisk (D) within the region.

Dam and Lees Ferry downstream (Plate 1). The canyon rim is at 300 m, on average, above the river and 1,220 m of elevation. The average annual temperature is 15.5 °C (National Park Service, 2014), and mean annual precipitation is less than 15.2 cm (National Park Service, 2014). Rainfall mostly occurs during the summer/fall period of the North American monsoon season.

The Glen Canyon Dam was completed in spring 1963. As a result, the Colorado River flow changed from a pattern of seasonal spring snowmelt flood to a pattern of daily disturbance associated with the regulated flow regime (Topping *et al.*, 2000) with major implications for riparian vegetation (Sankey *et al.*, 2015a). The post-dam reduction in flooding allowed for plant colonization of eddy sandbars and channel-margin deposits, and the expansion of riparian vegetation including tamarisk into the pre-dam active channel. Non-tamarisk riparian species include baccharis (*Baccharis spp.*), coyote willow (*Salix exigua*), common reed (*Phragmites australis*), western honey mesquite (*Prosopis glandulosa*), netleaf hackberry (*Celtis reticulata*), grey oak (*Quercus turbinella*), saltbush (*Atriplex canescens),* snakeweed (*Gutierrezia sarothrae),* and desert olive (*Forestieria neomexicana*).

Remote Sensing Data

We use aerial images acquired on 25-26 May in 2009 and 2013, respectively, with an ADS40 SH52 push-broom multispectral sensor mounted on a fixed-wing airplane (Davis, 2012). The 2009 data were acquired prior to any reported observations of beetle impacts on tamarisk within the study area and were, therefore, considered a "pre-beetle" dataset. The 2013 data were considered "post-beetle." Each multispectral image included four 12-bit spectral bands: blue (0.430-0.490 nm), green (0.535-0.585 nm), red (0.610-0.660 nm), and near-infrared (0.835-0.885 nm) with 20 cm spatial resolution spanning the entire segment of the river corridor and rim to rim across the canyon (Plate 1). A single multispectral image mosaic that spanned the study area was created for 2009 and 2013, respectively (Plate 1).

The lidar data were acquired on 10 July 2013 with a laser scanner mounted on a helicopter flying at approximately 200 m altitude above the river floodplain (Collins *et al.*, 2014). The lidar point cloud data (Plate 1) had an average density of 100 points/m^2 with total absolute horizontal and vertical error of 8 and 5 cm, respectively (Collins *et al.*, 2014).

Mapping Foliated and Defoliated Tamarisk with Multispectral Imagery

We first classified tamarisk that were vigorous and green (foliated) in 2009, but less so (defoliated) in 2013. To do this, we classified the 2009 multispectral imagery with the Mahalanobis Distance method in ENVI software (ENVI Version 4.8, ITT Industries Inc., 2010, Boulder, Colorado). The classification was calibrated with 1,500 training pixels and validated with another 1,500 pixels. The training and validation pixels were generated from 66 and 33 field-mapped tamarisk polygons, respectively, which were randomly designated as training or validation polygons. The tamarisk polygons were located and mapped in the field using large scale maps at a ratio of 1:756. The validation results indicated 79 percent overall accuracy (user's and producer's accuracies of 79 percent and 79 percent for tamarisk, respectively). Within the areas classified as tamarisk, greenness in 2009 was estimated by calculating the normalized difference vegetation index (NDVI). Changes in greenness from 2009 and 2013 was then estimated using the ratio of 2009 NDVI and 2013 NDVI. In 2009, pre-beetle tamarisk trees were still vigorous and expected to have relatively large NDVI values. A total of 40 individual, vigorous tamarisk trees within the study area in the 2009 imagery were spectrally examined and it was determined that they all had NDVI >0.35. Furthermore, known tamarisk patches were spectrally examined to confirm that their NDVI values on average were also >0.35. This site-specific threshold was then used to extract all pixels in the 2009 classification that had NDVI > 0.35 to represent healthy and vigorous tamarisk.

From 2009 to 2013, the NDVI values for tamarisk stands were expected to decline substantially due to defoliation by the tamarisk beetle. The tamarisk in the study area typically green up in early spring (e.g., March) and shed their leaves in late fall (e.g., October-November). The time period from late-May to early-July, when the remote sensing datasets were acquired, was the season when tamarisk canopies would typically be flush with green photosynthetically active leaves. However, while this was clearly the case for the 2009 pre-beetle data, large stands of tamarisk were obviously defoliated in the 2013 data. Due to the time of year, the defoliation is reasonably attributed to tamarisk beetle impacts which could include recent herbivory in April or May of that year and could also include derivative effects of herbivory in previous years since 2009. The NDVI ratio values between 2009 and 2013 were heuristically examined across the study area and a site-specific ratio (2009/2013) greater than 1.5 was determined within obvious areas of defoliation within the 2013 imagery. The ratio was conservatively established in order to not include tamarisk that were partially defoliated and other vegetation that had reduced in vigor due to other causes.

In the final map, defoliated tamarisk pixels met three criteria: (a) classified as tamarisk in the 2009 image with the Mahalanobis Distance classification, (b) NDVI >0.35 in 2009, and (c) 2009/2013 NDVI ratio greater than 1.5. The classification and final maps were further constrained to the previously mapped area of total riparian vegetation (i.e., includes all species) (Sankey *et al.*, 2015a; *https://www.sciencebase.gov/catalog/item/5575b3c1e4b08f9309d4bafc*). The defoliated tamarisk classification accuracy (Story and Congalton, 1986) was assessed using a total of 845 tamarisk points and 763 non-tamarisk points, which were randomly generated and field-validated in 2014 within tamarisk and non-tamarisk stands of riparian vegetation located throughout the study area.

Estimating Tamarisk Biomass with Lidar

Lidar ground returns and vegetation returns in the point cloud data were first separated using height filtering in ENVI software (Sankey *et al.*, 2013; Sankey *et al.*, 2015b; *https://bcal.boisestate.edu/tools/lidar*) and a vegetation canopy height model was created as a 0.5 m resolution raster. The subsequent analyses were then constrained to the pixels with canopy height > 2.9 m to focus on mature tamarisk, following Evangelista et al. (2007) who used 3 m as a threshold to identify mature tamarisk in their study and allometric models of tamarisk biomass. This height threshold excluded immature tamarisks that occur throughout our study area.

The canopy height model was segmented to delineate individual tree canopies and stands of merging trees using the ENVI segmentation tool with a population minimum of four 0.5 m pixels (equivalent to a minimum canopy diameter of 1 m). The segmented image was then overlaid with 10 m x 10 m grids, in which each square grid equaled a ground area of 100 m^2 following Evangelista *et al.* (2007) and their field plot size (100 m^2). The total canopy area within each grid was then calculated by summing the number of pixels with the segmented tree canopies and multiplying them by the grid area (Evangelista *et al.*, 2007). The canopy area estimates were then log-transformed (Evangelista *et al.*, 2007) and stacked with the maximum vegetation height image.

The resulting two band image was used to estimate average total aboveground tamarisk biomass (TAGB; kg) per m^2 area via the best (lowest Akaike Information Criteria) allometric regression model among five models published by Evangelista

et al. (2007):

$$\text{Log}_{10}(\text{TAGB}) = -1.1993 + 1.1090\ \text{Log}_{10}(\text{CA}) + 0.8595\ (\text{HT}) - 0.0927\ (\text{HT})^2 \quad (1)$$

where CA is the lidar-derived canopy area and HT is the lidar-derived canopy height. Since the model predicted a log-transformed TAGB, the resulting single band image was transformed back to TAGB. Furthermore, the allometric regression model had a correction factor to take into account a bias introduced by the log-log regression models (Evangelista *et al.*, 2007). The predicted TAGB by the model was, therefore, multiplied by the correction factor of 1.17 (Evangelista *et al.*, 2007).

Evangelista *et al.* (2007) determined that on average, 9.3 percent of the TAGB of an individual tamarisk tree is green foliage. In summer 2013, we sampled 40 tamarisk trees with evidence of defoliation within our study area, and estimated that on average 66.5 percent of the individual canopies (+- SE of 0.5 percent) were defoliated and the remainder of each canopy was green and leafed out. The proportion of TAGB that was green biomass remaining on the canopy was, therefore, estimated as:

$$\text{TAGB}_{\text{glpresent}} = 0.335*0.093*\text{TAGB}. \quad (2)$$

The proportion of the green leaf biomass potentially lost from the canopy due to defoliation was estimated as:

$$\text{TAGB}_{\text{glabsent}} = 0.665*0.093*\text{TAGB}. \quad (3)$$

The uncertainties of the TAGB, $\text{TAGB}_{\text{glpresent}}$, and $\text{TAGB}_{\text{glabsent}}$ estimates were determined using a Monte Carlo simulation approach adapted from recent forest and woodland remote sensing studies (Sankey *et al.*, 2013) that accounts for uncertainties in the remote sensing measurements, allometric regression equations and related field measurements, and spatial autocorrelation. A total of 100 realizations were calculated for each of the following equations with error terms:

$$\text{TAGB} = \text{CF}*10\text{^}[E_{\text{AlloReg}} + E_{\text{AlloReg}}*\text{LI} - 1.1993 + 1.1090*\text{Log}_{10}(\text{CA}+E_{\text{CA}}) + 0.8595\ (\text{HT}+E_{\text{HT}}) - 0.0927\ (\text{HT}+E_{\text{HT}})^2] \quad (4)$$

$$\text{TAGB}_{\text{glpresent}} = [0.35*0.093+E_{\text{leafb}}]*\text{CF}*10\text{^}[E_{\text{AlloReg}} + E_{\text{AlloReg}}*\text{LI} - 1.1993 + 1.1090*\text{Log}_{10}(\text{CA}+E_{\text{CA}}) + 0.8595\ (\text{HT}+E_{\text{HT}}) - 0.0927\ (\text{HT}+E_{\text{HT}})^2] \quad (5)$$

$$\text{TAGB}_{\text{glabsent}} = [0.65*0.093+E_{\text{leafb}}]*\text{CF}*10\text{^}[E_{\text{AlloReg}} + E_{\text{AlloReg}}*\text{LI} - 1.1993 + 1.1090*\text{Log}_{10}(\text{CA}+E_{\text{CA}}) + 0.8595\ (\text{HT}+E_{\text{HT}}) - 0.0927\ (\text{HT}+E_{\text{HT}})^2] \quad (6)$$

where CF is the correction factor (1.17) applied after taking the antilog of TAGB in Evangelista *et al.* (2007), E_{AlloReg} is an error term estimated from the standard error of the allometric regression equation in Evangelista *et al.* (2009), LI is the local Moran's *I* of TAGB (estimated without error terms) determined for a 1-pixel lag, E_{ca} is an error term estimated from the standard error of lidar-derived canopy area estimates (using standard error values published in Sankey *et al.*, 2013), E_{HT} is an error term estimated from the standard error of lidar-derived canopy height estimates (using standard error values published in Sankey *et al.*, 2013), E_{leafb} is an error term for leaf biomass estimated from the standard error of the percent canopy defoliation for the trees we sampled. We then produced and analyzed maps of the median and standard deviation of the 100 realizations of TAGB (Plate 2), $\text{TAGB}_{\text{glpresent}}$, and $\text{TAGB}_{\text{glabsent}}$ within those areas of the floodplain classified as defoliated tamarisk in 2013.

Results

Multispectral Image Classification

The multispectral image-derived classification of defoliated tamarisk in 2013 had an overall accuracy of 86.1 percent. Producer's accuracies were 91.2 percent and 80.6 percent for defoliated tamarisk and non-tamarisk stands, respectively. User's accuracies were 83.9 percent and 89.2 percent, respectively, for these two classes (Table 1). The map classified 24.7 percent of the tamarisk area in Glen Canyon as defoliated tamarisk, which is equivalent to 49,408 m^2 area along the river floodplain.

TABLE 1. ACCURACY ASSESSMENT OF THE DEFOLIATED TAMARISK VERSUS NON-TAMARISK CLASSIFICATION USING THE MULTISPECTRAL IMAGERY

	Reference Data			
Classification	Defoliated tamarisk	Non-tamarisk	Total	User's accuracy
Defoliated tamarisk	771	148	919	**84%**
Non-tamarisk	74	615	689	**89%**
Total	845	763	1608	
Producer's accuracy	**91%**	**81%**		
Overall accuracy			**86%**	

Lidar-derived Tamarisk Biomass

The mean TAGB was 2.17 kg (SD=4.41) per 0.5-m pixel and 8.68 kg/m^2 (Plate 2). The mean $\text{TAGB}_{\text{glpresent}}$ with the remaining green biomass was 0.07 kg (SD = 0.15) per 0.5 m pixel and 0.28 kg/m^2. The mean $\text{TAGB}_{\text{glabsent}}$ was 0.13 kg (SD = 0.28) per pixel and 0.52 kg/m^2, which indicated an equivalent of 25,692 kg of tamarisk leaf biomass potentially shed over the entire area of the river floodplain (Plate 3).

Discussion

Mapping Tamarisk with Multispectral Data

We produced a highly accurate classification map of defoliated tamarisk along the Colorado River in Glen Canyon National Recreation Area, Arizona. The riparian study area is located within a deep, narrow canyon that is world-renown for its extremely complex topography. As a result, many of the tamarisk stands are distributed in small patches along the narrow stretches of riparian floodplain. The small patches in the narrow canyon are difficult to detect, especially in dark shadows that can occur due to the steep canyon walls. Unlike other areas, satellite data and other common image sources are not suitable for remote sensing applications along the Colorado River throughout the Grand Canyon region due to the complex topography. Furthermore, previous tamarisk remote sensing studies indicate that tamarisk is spectrally challenging to distinguish from the native vegetation, even when using high spatial resolution satellite imagery such as AVIRIS (4 m pixel) and QuickBird (2.5 m pixel) (DiPietro *et al.*, 2002; Carter *et al.*, 2009; Hamada *et al.*, 2007; Xun and Wang, 2015). Similar to other tamarisk remote sensing studies (Anderson *et al.*, 2005; Hamada *et al.*, 2007; Xun and Wang, 2015), we attribute much of the success of our classification to the high spatial resolution (20 cm) of the multispectral data. The accuracies observed in this study are similar to those found in other tamarisk studies using hyperspectral image classification in less complex terrain (Carter *et al.*, 2009; Hamada *et al.*, 2007).

We had the unique opportunity to leverage pre-beetle and

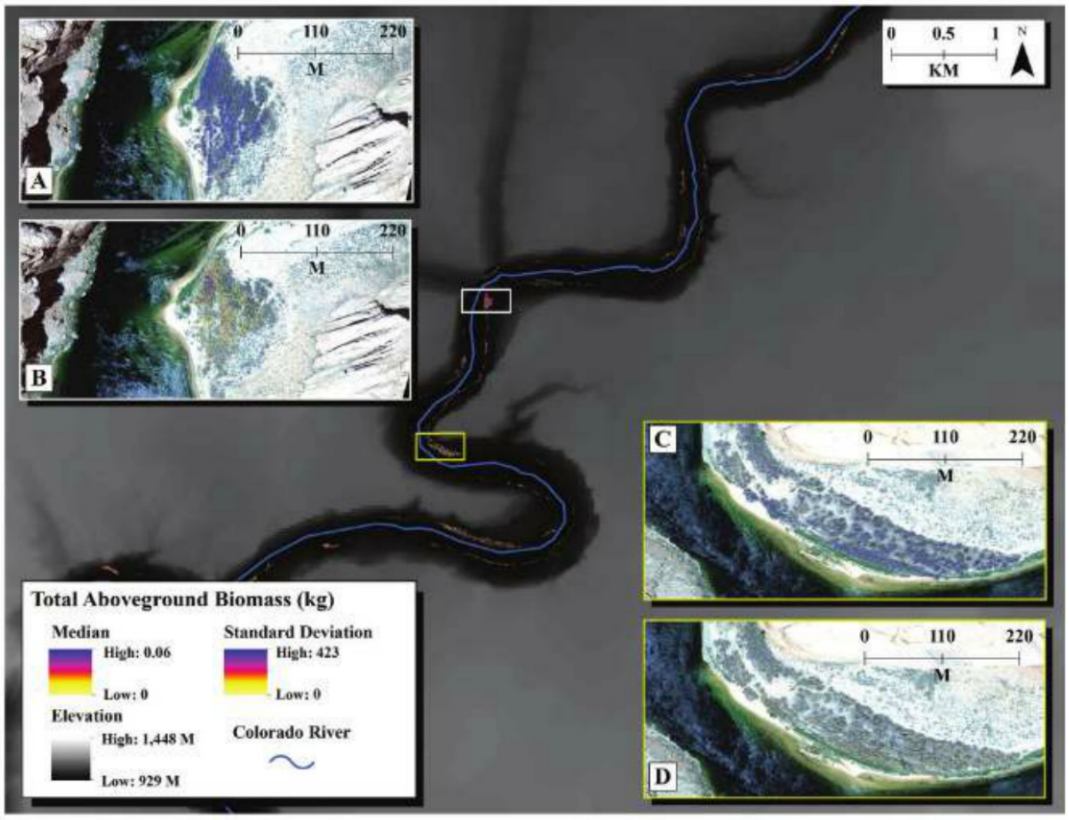

Plate 2. Tamarisk total aboveground biomass (TAGB) within the defoliated tamarisk stands in our study area estimated using fusion of lidar and multitemporal multispectral data. Insets are examples of the median and standard deviation of TAGB overlaid on the multispectral image at Ferry Swale (Panels A and B, respectively) and Nine-Mile (Panels C and D, respectively) recreation sites within Glen Canyon National Recreation Area.

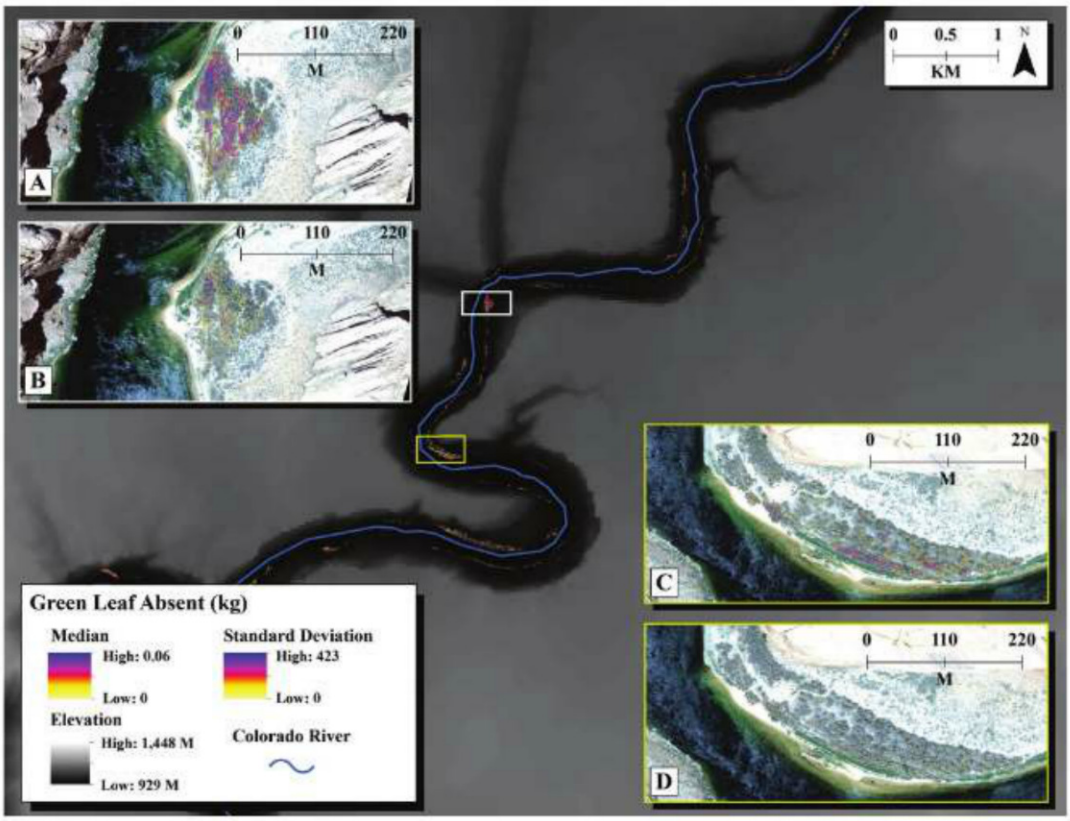

Plate 3. Tamarisk green leaf biomass potentially lost from the canopy due to defoliation ($TAGB_{glabsent}$) within the defoliated tamarisk stands in our study area. Insets are examples of the median and standard deviation of $TAGB_{glabsent}$ overlaid on the multispectral image at Ferry Swale (Panels A and B, respectively) and Nine-Mile (Panels C and D, respectively) recreation sites within Glen Canyon National Recreation Area.

post-beetle multitemporal data in detecting defoliated tamarisk. Much of the beetle effect monitoring is performed using expensive and labor-intensive field measurements (Everitt and Deloach, 1990; Hamada *et al.*, 2007). Similar to previous tamarisk studies (Dennison *et al.*, 2009; Fletcher, 2013; Nagler *et al.*, 2012; Snyder *et al*, 2010), we focused on the expected decrease in photosynthetic activity, which we approximated as a 1.5-fold decrease in NDVI at our study site between 2009 and 2013. Consistent with previous tamarisk impact studies (Bateman *et al.*, 2013; Hultine *et al*, 2010; Nagler *et al.*, 2012; Snyder *et al.*, 2010), our estimates indicate that a large portion of the tamarisk population defoliated along the Colorado River between the Glen Canyon Dam and Lees Ferry over the study period. It is important to note that the defoliation is likely due to a combination of repeat episodes of beetle herbivory, as well as annual defoliation that occurs physiologically irrespective of herbivory.

In a recent review of tamarisk and the beetle interactions, Nagler and Glenn (2013) highlight that the tamarisk beetle herbivory is most effective in the initial years following the beetle arrival and during the population expansion leading to 50 to 75 percent tamarisk leaf reduction, but the trend can change within a few more years. Nagler and Glenn (2013) further indicate that the tamarisk beetle effects are ecosystem-specific. Our study provides the first spatially-explicit estimate of tamarisk beetle effects in Glen Canyon to our knowledge, which can be used as a benchmark estimate in future monitoring. Continued monitoring, especially in a unique ecosystem such as the Glen Canyon and Grand Canyon region, are essential to efficiently guide restoration management (Lindenmayer, 1999). Tamarisk and the beetle interactions are still developing in the western US (Nagler and Glenn, 2013) and the eventual equilibrium of the two species at the ecosystem level and their cascading trophic effects are currently unknown (Carter *et al.*, 2009). As these interactions develop over time, continued remote monitoring of tamarisk and the beetle distribution can inform adaptive management at the landscape scale and restoration activities.

Lidar-Derived Estimates of Tamarisk Biomass and Defoliation

We integrated very high spatial resolution lidar data with the multitemporal, multispectral imagery to estimate several important components of biomass, and uncertainties therein, for individual defoliated tamarisk trees throughout the study area. Our methods, maps, and estimates of tamarisk biomass provide an important practical tool for land managers, both in our study area as well as similar riparian systems around the world. In this and other riparian ecosystems, tamarisk has invaded and overgrown areas of native riparian vegetation, which has clogged sandbars and channel margins used by river runners, fisherman, and other recreationalists (Shafroth *et al.*, 2005).

In areas of greater mortality due to herbivory, managers are confronting a fire danger in the dead standing and fallen tamarisk. The dead standing tamarisk also reduce the aesthetic and recreational value of the canyon, which is generating even greater impetus for biomass removal treatments (O'Meara *et al.*, 2009). Managers working within proposed areas for tamarisk reduction can use our TAGB estimates and maps to identify and spatially target the amount of biomass that would need to be removed either mechanically, or consumed as fuel in a prescribed fire, or treated with herbicide. Controlled floods might also be considered as a management tool (Nagler and Glenn, 2013; O'Meara *et al.*, 2009). In such scenarios, our TAGB estimates identify areas of high degree of defoliation that are within the contemporary flood stage and have potential for tamarisk removal with the use of controlled floods.

In comparison to the previous tamarisk studies using satellite images and image-derived NDVI and EVI (Dennison *et al.*, 2009; Ji and Wang, 2015; 2016; Nagler *et al.*, 2005; Nagler *et al., 2008*; Nagler *et al.*, 2014; Meng *et al.*, 2012), our lidar-derived TAGB estimates with and without the leaves have much higher spatial resolution and illustrate the local-scale variability in tamarisk defoliation. This is essential for targeting restoration activities to spatially-variable conditions along the river corridor. Previous studies have demonstrated that the ecological impacts of tamarisk defoliation are site-specific leading to varied density and population of fauna, invertebrates, mammals, and birds. Consequently, the US Department of Agriculture has banned further release of the biocontrol beetle due to the currently unknown and varying Tamarisk-Beetle-Avian interactions, in particular concerning the endangered southwestern willow flycatcher, a riparian-obligate bird, who has adapted to tamarisk as a replacement habitat (Nagler and Glenn, 2013). Our high-resolution TAGB estimate can help understand such relationships and their spatial variability. Our estimates of $TAGB_{glabsent}$ can also help understand the implications of defoliation on net evapotranspiration, ecosystem carbon, and nutrient cycling.

Tamarisk is known to have high leaf nitrogen (N) content and higher rates of leaf litter decomposition relative to some native riparian species (Hultine *et al.*, 2010). Thus, the high N litter that accumulates due to beetle defoliation could easily infiltrate into the riparian soil profile, as well as be exported downstream in the mainstem river flow. Our $TAGB_{glabsent}$ methods, and estimates can be used to estimate potential allocthonous inputs into the riparian system using litter, organic matter, and nutrient fluxes from biomass lost from tree canopies due to defoliation events (Kennedy and Hobbie, 2004; Kennedy and Ralston, 2012). For example, total aboveground tamarisk biomass was 8.68 kg/m^2 (SD = 17.6), on average, and $TAGB_{glabsent}$ estimates indicate that defoliation by tamarisk beetle, potentially at a higher frequency than the annual phenological leaf shedding, resulted in a mean leaf biomass loss of 0.52 kg/m^2: an equivalent of 25,692 kg of tamarisk leaf biomass shed across the entire study area. In comparison, Kennedy and Ralston (2012) suggested that mean annual tamarisk litter production for the Colorado River downstream of Glen Canyon Dam prior to introduction of the tamarisk leaf beetle was 0.30 kg/m^2 (95 percent confidence interval = 0.18–0.42 kg/ m^2; also see Kennedy and Hobbie, 2004). Litter chemistry measurements (n = 15) collected several months after our 2013 imagery and lidar acquisitions indicates that the tamarisk litter was on average 1.22 percent N (SE = 0.087 percent). While acknowledging that total N is larger than the amount of available N in tamarisk litter at any given time, we nonetheless estimate that, within the study area at the time of the remote sensing data acquisitions, there might have been as much as 313 kg of N stored in tamarisk leaf litter. Over the course of decomposition, this N will infiltrate into the floodplain soil profile and/or the flow of the river. In this and other study areas where additional multitemporal datasets can be acquired strategically to target specific time periods, the potential differences in allocthonous inputs due to individual defoliation events associated with insect herbivory or annual defoliation might be isolated and examined independently.

Conclusions

Using high-resolution multitemporal, multispectral data, we classified tamarisk defoliation in the Glen Canyon area in Arizona. The high spatial resolution classification provides key information to effectively inform restoration treatments regarding where and how much mechanical removal or controlled burning could be performed. Furthermore, the defoliated tamarisk classification can help understand the site-specific and spatially-variable relationship between

tamarisk and the tamarisk beetle at this critical stage when their interactions are still developing and currently unknown. We suggest continued high-resolution remote monitoring of the interactions as the eventual equilibrium between the species and the cascading effects unfold in the region. Our lidar-derived approach to estimating TAGB with and without the leaves may provide crucial insight to the cascading effects of the tamarisk beetle on ecosystem processes, including net evapotranspiration, C fluxes, and nutrient cycles. Such effects could be considered before large-scale restoration treatments are conducted.

Acknowledgments

This work was funded by the U.S. Department of the Interior Bureau of Reclamation through the Glen Canyon Dam Adaptive Management Program. The authors wish to thank: Barbara Ralston for discussions that helped conceive the study, and for assisting with field work; Sasha Reed for completing the leaf/litter chemistry analysis and for helpful review of an earlier draft of the manuscript; Charles Yackulic for helpful discussions that improved the statistical analyses; Laura Cagney for helpful reviews of the remote sensing data products; Pamela Nagler for providing the USGS internal manuscript review; Terry Arundel and Brad Davis for assistance with the data processing. Any use of trade, product, or firm names is for descriptive purposes only and does not imply endorsement by the U.S. Government. We also thank Northern Arizona University (NAU)/NASA Space Grant Undergraduate Internship Program for supporting the undergraduate researcher and author, Rene Horne.

References

Anderson, G.L., R.I. Carruthers, G.E. Shaokui, and P. Gong, 2005. Monitoring of invasive *Tamarix* distribution and effects of biological control with airborne hyperspectral remote sensing, *International Journal of Remote Sensing*, 26:2487–2489.

Bateman, H.L., P.L. Nagler, and E.P. Glen, 2013. Plot- and landscape-level changes in climate and vegetation following defoliation of exotic saltcedar (*Tamarix* sp.) from the biocontrol agent *Diorhabda carinulata* along a stream in the Mojave Desert (USA), *Journal of Arid Environments*, 89:16–20.

Bean, D., T. Dudley, and J. Keller, 2007. Seasonal timing of Diapause induction limits the effective range of *Diorhabda elongate deserticola* (*Coleoptera*: *Chrysomelidae*) as a biological control agent for Tamarisk (*Tamarix* spp.), *Environmental Entomology*, 36:15–25.

Bateman, H.L., P.L. Nagler, and E. P. Glenn, 2013. Plot- and landscape-level changes in climate and vegetation following defoliation of exotic saltcedar (*Tamarix* so.) from the biocontrol agent *Diorhabda carinulata* along a stream in the Mojave Desert (USA), *Journal of Arid Environments*, 89:16–20.

Bateman, H.L., D.M. Merritt, E.P. Glenn, and P.L. Nagler, 2015. Indirect effects of biocontrol of an invasive riparian plant (Tamarix) alters habitat and reduces herpetofauna abundance, *Biological Invasions*, 17:87–97.

Carter, G.A., K.L. Lucas, G.A. Blossom, C.L. Lassitter, D.M. Holiday, D.S. Mooneyhan, D.R. Fastring, T.R. Holcombe, and J.A. Griffith, 2009. Remote sensing and mapping of tamarisk along the Colorado River, USA: A comparative use of summer-acquired Hyperion, Thematic Mapper and Quickbird Data, *Remote Sensing*, 1:318–329.

Collins, B.D., Corbett, S.C., Sankey, J.B., and H.C. Fairley, 2014. High-resolution topography and geomorphology of select archeological sites in Glen Canyon National Recreation Area, Arizona, *U.S. Geological Survey Scientific Investigations Report 2014–5126*, 31 p. URL: *http://dx.doi.org/10.3133/sir20145126* (last date accessed: 16 June 2016).

Crins, W.J, 1989. The Tameraceae in the Southwestern United States, *Journal of the Arnold Arboretum*, 70:403–425

Cross, W., C. Baxter, K. Donner, E. Rosi-Marshall, T. Kennedy, R. Hall, H. Wellard Kelly, and R. Rogers, 2011. Ecosystem ecology meets adaptive management: Food web response to a controlled flood on the Colorado River, Glen Canyon, *Ecological Applications*, 21:2016–2033

Davis, P.A., 2012, Airborne digital-image data for monitoring the Colorado River corridor below Glen Canyon Dam, Arizona, 2009 - Image-mosaic production and comparison with 2002 and 2005 image mosaics, *U.S. Geological Survey Open-File Report 2012–1139*, URL: *http://pubs.usgs.gov/of/2012/1139/* (last date accessed: 16 June 2016).

DeLoach, J., P. Lewis, J. Herr, R. Carruthers, J. Tracy, and J. Johnson, 2003. Host specificity of the leaf beetle, *Diorhabda elongata deserticola* (*Coleoptera: Chrysomelidae*) from Asia, a biological control agent for saltcedars (*Tamarix: Tamaricaceae*) in the Western United States, *Biological Control*, 27(2):117–147.

Dennison, P.E., P.L. Nagler, K.R. Hultine, E.P. Glenn, and J.R. Ehleringer, 2009. Remote monitoring of tamarisk defoliation and evapotranspiration following saltcedar leaf beetle attack, *Remote Sensing of Environment*, 113:1462–1472

DiPietro, D., S. Ustin, and E. Underwood, 2002. Mapping the invasive plant *Arundo donax* and associated riparian vegetation using AVIRIS, *Proceedings of 2002 Airborne Visible/Infrared Imaging Spectrometer (AVIRIS) Workshop*, Pasadena, California: NASA JPL.

DiTomaso, J., 1998. Impact, biology, and ecology of saltcedar (*Tamarix* spp.) in the southwestern United States, *Weed Technology*, 12:326–336.

Dudley, T., 2005. Progress and pitfalls in the biological control of saltcedar (Tamarisx Spp.) in North America, *Proceedings of the 16th U.S Department of Agriculture Interagency Research Forum on Gypsy Moth and Other Invasive Species*, pp. 12

Dudley, T.L., D.W. Bean, R.R. Pattison, and A. Caires, 2012. Selectivity of a biological control agent, *Diorhabda carinulata Desbrochers*, 1870 (Coleoptera: Chrysomelidae) for host species within the genus *Tamarix Linneaus*, 1753, *The Pan-Pacific Entomologist*, 88:319–341

Evangelista, P., S. Kumar, T. Stohlgren, A. Crall, and G. Newman, 2007. Modeling aboveground biomass of *Tamarix ramosissima* in the Arkansas river basin of southeastern Colorado, USA, *Western North American Naturalist*, 67:503–509.

Everitt, J.H., and C.J. Deloach, 1990. Remote sensing of Chinese tamarisk (*Tamarix chinensis*) and associated vegetation, *Weed Science*, 38:273–278.

Fletcher, R., 2013. Employing spatial information technologies to monitor biological control of saltcedar in West Texas, *Geocarto International*, 29:332–347

Glenn, E.P., K. Morion, P.L. Nagler, R.S. Murray, S. Pearlstein, K.R. Hultine, 2012. Roles of saltcedar (Tamairx spp.) and capillary rise in salinizing a non-flooding terrace on a flow-regulated desert river, *Journal of Arid Environments*, 79:56–65

Hamada, Y., D.A. Stow, L.L. Coulter, J.C. Jafolla, and L.W. Hendricks, 2007. Detecting Tamarisk species (*Tamarix* spp.) in riparian habitats of southern California using high spatial resolution hyperspectral imagery, *Remote Sensing of Environment*, 109:237–248.

Hart, C., 2009. *Saltcedar: Biology and Management*, The Texas Water Resources Institute of Texas A&M, Texas A&M System, L-5440

Hultine, K., J. Belnap, C. van Riper III, J. Ehleringer, P. Dennison, M. Lee, P. Nagler, K. Snyder, S. Uselman, and J. West, 2010a. Tamarisk biocontrol in the western United States: Ecological and societal implications, *Ecology and Environ*ment, 8:467–474.

Hultine, K.R., P.L. Nagler, K. Morino, S.E. Bush, K.G. Burtch, P.E. Dennison, E.P. Glenn, and J.R. Ehleringer, 2010b. Sap flux-scaled transpiration by tamarisk (*Tamarix* spp) before, during and after episodic defoliation by the saltcedar leaf beetle (*Diorhabda carinulata*), *Agricultural and Forest Meteorology*, 150:1467–1475.

Infalt, S.B., 2005. Colorado River native riparian vegetation in Grand Canyon: How has Glen Canyon Dam impacted these communities?, *University of California Davis, Department of Geology*.

Ji, W., and L. Wang, 2015. Discriminating saltcedar (*Tamarix ramosissima*) from sparsely distributed cottonwood (*Populus euphratica*) using a summer season satellite image, *Photogrammetric Engineering & Remote Sensing*, 81(8):795–806.

Ji, W., and L. Wang, 2016. Phenology-guided saltcedar (Tamarix spp.) mapping using Landsat TM images in western US, *Remote Sensing of Environment*, 173:29–38.

Jorgensen, M., 1996. The use of prescribed fire and mechanical removal as means of control of Tamarisk trees, *Proceedings of the 1996 Saltcedar Management Workshop*.

Kennedy T.A., and S.A. Hobbie, 2004. Saltcedar (*Tamarix remosissima*) invasion alters organic matter dynamics in a desert stream, *Freshwater Biology*, 49:65–76.

Kennedy, T.A., and B.E Ralston, 2012. Regulation leads to increases in riparian vegetation, but not direct allochthonous inputs, along the Colorado River in Grand Canyon, Arizona, *River Research and Applications*, 28:2–12. doi:10.1002/rra.1431.

Ladenburger, C.G., A.L. Hild, D.J. Kazmer, and L.C. Munn, 2006. Soil salinity patterns in *Tamarix* invasions in the Bighorn Basin, Wyoming, USA, *Journal of Arid Environments*, 65:111–128

Lindenmayer, D.B., 1999. Future directions for biodiversity conservation in managed forests: Indicator species, impact studies and monitoring programs, *Forest Ecology and Management*, 115:277–287

Meng, R., P.E. Dennison, L.R. Jamison, C. van Riper III, P. Nagler, K.R. Hultine, D.W. Bean, and T. Dudley, 2012. Detection of tamarisk defoliation by the northern tamarisk beetle based on multitemporal Landsat 5 Thematic Mapper imagery, *GIScience and Remote Sensing*, 49:510–537.

Meng, R., and P.E. Dennison, 2015. Spectroscopic analysis of green, dessicated, and dead tamarisk canopies, *Photogrammatric Engineering & Remote Sensing*, 81:199–207.

Merritt, D.M., and P.B. Shafroth, 2012. Edaphic, salinity, and stand structure trends in chronosequences of native and non-native dominated riparian forests along the Colorado River, USA, *Biological Invasions*, 14:2665–2685.

Nagler, P., E. Glenn, C. Curtis, K. Schiff-Hursh, and A. Huete, 2005. Vegetation mapping for change detection on an arid-zone river, *Environmental Monitoring and Assessment*, 109:255–274.

Nagler, P., E.P. Glenn, K. Didan, J. Osterberg, F. Jordan, and J. Cunningham, 2008. Wide-area estimates of stand structure and water use of *Tamarix* spp. on the Lower Colorado River: Implications for restoration and water management projects, *Restoration Ecology*, 16:136–145.

Nagler, P., E.P. Glenn, C.S. Jarnevich, and P.B. Shafroth, 2011. Distribution and abundance of saltcedar and Russian olive in the Western United States, *Critical Reviews in Plant Sciences*, 30:508–523.

Nagler, P., T. Brown, K.R. Hultine, C. van Riper III, D.W. Bean, P.E. Dennison, R.S. Murray, and E.P. Glenn, 2012. Regional scale impacts of Tamarix leaf beetles (*Diorhabda carinulata*) on the water availability of western US rivers as determined by multi-scale remote sensing methods, *Remote Sensing of Environment,* 118:227–240.

Nagler, P., and E. Glenn, 2013. *Tamarix* and *Diorhabda* leaf beetle interactions: Implications for *Tamarix* water use and riparian habitat, *Journal of the American Water Resources Association*, 49:534–548.

Nagler, P., S. Pearlstein, E.P. Glenn, T.B. Brown, H.L. Bateman, D.W. Bean, and K.R. Hultine, 2014. Rapid dispersal of saltcedar (*Tamarisk* spp.) biocontrol beetles (*Diorhabda carinulata*) on a desert river detected by phenocams, MODIS imagery and ground observations, *Remote Sensing of Environment*, 140:206–219.

O'Meara, S., D. Larsen, and C. Owens, 2010. Methods to control saltcedar and Russian olive, *Saltcedar and Russian Olive Control Demonstration Act Science Assessment* (P.B. Shafroth, C.A. Brown, and D.M. Merritt, editors), *U.S. Geological Survey Scientific Investigations Report 2009-5247*, pp. 65–102.

Ohrtman, M.K., A.A. Sher, and K.D. Lair, 2012. Quantifying soil salinity in areas invaded by *Tamarix* spp, *Journal of Arid Environments*, 85:114–121.

Pattison, R., C. D'Antonio, T. Dudley, K. Allander, and B. Rice, 2011. Early impacts of biological control on canopy cover and water use of the invasive saltcedar tree (*Tamarix* spp.) in western Nevada, USA, *Oecologia*, 165:605–616.

Paxton, E., T. Theimer, and M. Sogge., 2011. Tamarisk biocontrol using tamarisk beetles: Potential consequences for riparian birds in the Southwestern United States, *The Condor*, 113:255–265

Penny, R., 1991. *The Whitewater Sourcebook: A Directory of Information on American Whitewater Rivers*, Birmingham, Alabama, Menasha Ridge Press.

Sankey, J.B., B.E. Ralston, P.E. Grams, J.C. Schmidt, and L.E. Cagney, 2015a. Riparian vegetation, Colorado River, and climate: Five decades of spatio-temporal dynamics in the Grand Canyon with river regulation, *Journal of Geophysical Research*, 120:1532–1547. doi:10.1002/2015JG002991.

Sankey, J.B., S. Munson, R.H. Webb, C. Wallace, and C. Duran, 2015b. Remote sensing of Sonoran Desert vegetation structure and phenology with ground-based LiDAR, *Remote Sensing*, 7:342-359. doi: 10.3390/rs70100342.

Sankey, T.T., R. Shrestha, J.B. Sankey, S.H. Hardegree, and E. Strand, 2013. Lidar-derived estimate and uncertainty of carbon sink in successional phases of woody encroachment, *Journal of Geophysical Research - Biogeosciences*, 118:1144–1155. doi: 10.1002/jgrg.20088

Shafroth, P.B., J.R. Cleverly, T.L. Dudley, J.P. Taylor, C. Van Riper III, E.P. Weeks, and J.N. Stuart, 2005. Control of Tamarisk in the Western United States: Implications for water salvage, wildlife use and riparian restoration, *Environmental Management*, 35:231–246

Snyder, K., S. Uselman, T. Jones, and S. Duke, 2010. Ecophysiological responses of salt cedar (*Tamarix spp*. L.) to the northern tamarisk beetle (*Diorhabda carinulata* Desbrochers) in a controlled environment, *Biological Invasions*, 12:3795–3808.

Story, M., and R.G. Congalton., 1986. Accuracy assessment: A user's perspective, *Photogrammetric Engineering & Remote Sensing*, 52:397–399.

Topping, D.J., D.M. Rubin, and L.E. Vierra Jr., 2000. Colorado River sediment transport: 1. Natural sediment supply limitation and the influence of the Glen Canyon Dam, *Water Resources Research*, 36:515–542. doi:10.1029/1999WR900285.

Xun, L., and L. Wang, 2015. An object-based SVM method incorporating optimal segmentation scale estimation using Bhattacharyya Distance for mapping salt cedar (*Tamarisk* spp.) with QuickBird imagery, *GIScience & Remote Sensing*, 52:257–273.

(Received 15 October 2015; accepted 22 December 2015; final version 22 February 2016)